NANO LETTERS

pubs.acs.org/NanoLett

Quantum Linear Magnetoresistance in Multilayer Epitaxial Graphene

Adam L. Friedman,*,† Joseph L. Tedesco,‡ Paul M. Campbell,† James C. Culbertson,† Edward Aifer,§ F. Keith Perkins,† Rachael L. Myers-Ward,‡ Jennifer K. Hite,‡ Charles R. Eddy, Jr.,‡ Glenn G. Jernigan,|| and D. Kurt Gaskill‡

†Code 6876, ‡Code 6882, §Code 6818, and ||Code 6812, U.S. Naval Research Laboratory, Washington, D.C. 20375

ABSTRACT We report the first observation of linear magnetoresistance (LMR) in multilayer epitaxial graphene grown on SiC. We show that multilayer epitaxial graphene exhibits large LMR from 2.2 K up to room temperature and that it can be best explained by a purely quantum mechanical model. We attribute the observation of LMR to inhomogeneities in the epitaxially grown graphene film. The large magnitude of the LMR suggests potential for novel applications in areas such as high-density data storage and magnetic sensors and actuators.

KEYWORDS Graphene, epitaxial graphene, magnetoresistance, transport, gapless semiconductor, disordered systems

Normally, a conductor in an applied magnetic field responds with a quadratic magnetoresistance (MR) that saturates at low fields and displays a relatively small magnitude. However, creating inhomogeneities in the material can instead induce a large nonsaturating linear magnetoresistance (LMR). This was treated quantum mechanically[1,2] in various disordered thin films where there exists an approximately linear energy spectrum, carriers of very low effective mass, and an approximately zero bandgap. Interest in materials with LMR for device and sensor applications has recently been renewed[3] due to the discovery of new methods to create desirable traits in samples by the nanoscale manipulation of structure. LMR has been recently reported in MnAs-GaAs nanoparticles and films,[4] nonstoichiometric silver chalcogenides,[5−7] InSb,[8] and silicon.[9] Because of its unusual band structure with naturally zero bandgap and a linear dispersion,[10] graphene should provide the perfect platform for the study of LMR.[8]

This paper investigates LMR in multilayer epitaxially grown graphene devices for which the device size is much larger than the domain size of the material. Therefore, the devices are inherently disordered. For a disordered conductor displaying LMR, both quantum and classical routes to LMR can compete, that is, under certain conditions (such as different temperature regions) each model could explain the LMR of the same material, albeit not concurrently.[8] The revision of the older quantum models for LMR by Abrikosov[2] and the development of the classical model by Parish and Littlewood (PL model)[11−13] offer a thorough explanation of each subject. Despite predictions,[8] LMR has yet to be observed in graphene devices because the large amplitude of Shubnikov−de Haas oscillations (SdHO) and quantum Hall effect observed in clean, homogeneous exfoliated graphene (the current experimental standard[10,14]) are likely to overwhelm and obscure any linear dependence. However, epitaxially grown multilayer graphene devices can allow LMR observation because of their disorder. Here we show that the LMR data suggest that epitaxial graphene retains quantum character even to room temperature despite expectations that classical LMR would prevail.[8]

Multilayer epitaxial graphene was synthesized on semi-insulating, carbon face (000-1) 4H SiC wafers.[15,16] Devices were fabricated by employing standard photolithographic techniques with Hall bar patterns defined by oxygen plasma etching and ohmic contacts deposited by electron beam-assisted deposition and liftoff of Ti/Au. Low-temperature (4.2 K) magnetotransport measurements were conducted in a 13 T He-cooled superconducting magnet system and variable temperature (2.2−300 K) measurements were taken with a 9 T variable temperature He-cooled superconducting magnet system. Applied current for all measurements was 10 μA.

Figure 1A shows LMR in one sample at 4.2 K. Several devices were tested, and the peak MR_{xx} ($\Delta\rho/\rho$) varied from approximately 80−250% at 4.2 K and 12 T. ρ is the resistivity, $\Delta\rho$ is the change in resistivity with respect to the zero field value, and the subscript "xx" on MR refers to the longitudinal measurement configuration, while "xy" will later refer to the transverse configuration. We believe this to be one of the largest MRs reported in graphene sheets and that its magnitude may increase with further materials optimization by controlling the disorder more precisely. All longitudinal contact configurations displayed exactly the same LMR signal, thereby eliminating parallel conductance as a cause of the behavior.[17] SdHO were extracted from the data by averaging the positive and negative field sweep data and are displayed in Figure 1B. The SdHO attests to the quantum nature of LMR at this temperature.

* To whom correspondence should be addressed.
Received for review: 05/21/2010
Published on Web: 00/00/0000

DOI: 10.1021/nl101797d | *Nano Lett.* **XXXX,** *xxx,* 000–000

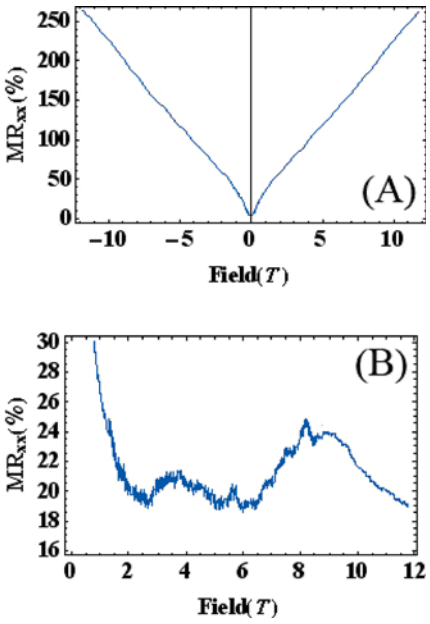

FIGURE 1. (A) LMR observed at 4.2 K with MR of 250% at 12 T. (B) SdHO extracted from the positive and negative field sweeps of the LMR.

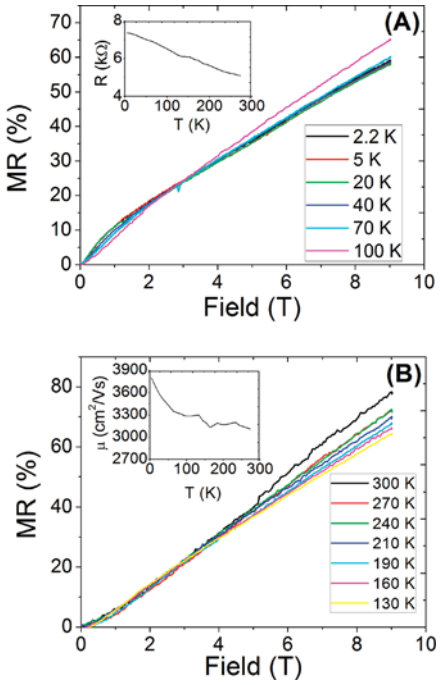

FIGURE 2. (A) The $T \leq 100$ K MR data. The data are almost temperature independent. The inset shows resistance vs temperature indicating the absence of phonon scattering and a band gap in the sample. (B) The $T > 100$ K data shows a change in inflection in the quadratic part of the MR and a slight increase in MR magnitude as a function of temperature. The inset shows the Hall mobility vs temperature.

Figure 2 shows the temperature dependent LMR in another sample. Curves for $T \leq 100$ K are displayed in Figure 2A while curves for higher temperature are displayed in Figure 2B. The change in the curves, or when the slope begins to increase and the inflection changes near the crossover field, H_c (the field at which the data become linear), at 100 K appears at a point at which the mobility seems to stabilize (see Figure 2B inset). According to past studies in other materials,[8] the change could indicate a switch from quantum to classical LMR behavior. Figure 2A shows that there is very little change for the low-temperature LMR. The MR is linear above approximately 1 T. The inset of Figure 2A shows the zero-field resistance versus temperature for the sample. The resistance decreases almost linearly with temperature indicating that there is no bangap, as a nonzero bandgap would show thermally activated behavior. More importantly, the LMR persists even up to room temperature, which to the best of our knowledge, is not evident in any other carbon-based material yet studied.

The inset of Figure 2B shows the Hall mobility as a function of temperature. We see that although the mobility decreases slightly with temperature, the magnitude is not strongly dependent on temperature. We also do not observe a significant change in electron density as a function of temperature. We therefore attribute the slight increase of mobility at lower temperatures to decreased phonon scattering. In Figure 2B, as the temperature increases for $T > 100$ K, the inflection of the data changes and the MR slowly increases with increasing temperature. There is no immediate explanation for this change in inflection, but it has been observed in other studies of LMR.[8] However, it is interesting to note that the slight increase in mobility for $T < 100$ K seems to correspond to this change in curvature. Therefore, the change of inflection may be attributable to mobility changes. Figure 3A shows the crossover field, or the field at which the MR becomes linear, as a function of temperature. Here, we see that the measured value of the crossover field oscillates around an average value of 1 T.

To ascertain the extent of inhomogeneity and sample thickness in devices, confocal Raman spectroscopy was performed. Figure 4 displays the results for one device tested (from which the data for Figure 2 were taken). Raman spectra of all devices tested revealed similar results. The inset of Figure 4 shows a Nomarski image of the device, and the corresponding spatial map of the attenuation of the substrate Raman signal (inset middle). The intensities of the substrate's Raman lines are attenuated by the presence of the graphene and thus can provide a measure of film thickness[18] (Figure 4, inset left). We find an average of 16 ± 3 nm (~50 graphene monolayers) in the tested devices. The film thickness, however, varies across the device. Raman signal originating from the graphene D and G lines are shown in Figure 4. Raman measurements of the ratio of intensity for the G (I_G) and D (I_D) lines can be correlated to an average grain size.[19] From this correlation, we determine that the average grain size in this film is ~1.5 μm, which is much smaller than the device length (~125 μm). Given the small grain size compared with the device size, the devices can be considered inhomogeneous.

DOI: 10.1021/nl101797d | *Nano Lett.* **XXXX,** *xxx,* 000–000

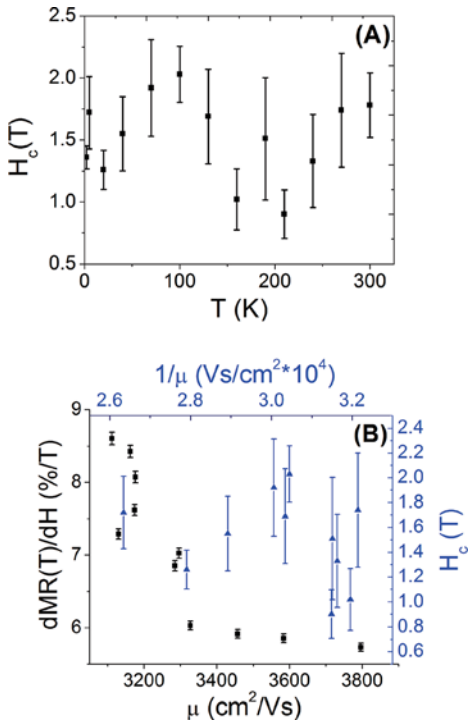

FIGURE 3. (A) The crossover field as a function of temperature. Error bars are standard deviation. (B) dMR(T)/dH vs μ (black squares; bottom and left axes) and Hc vs $1/\mu$ (blue triangles; top and right axes) should both show linear relationships (direct proportionality) according to the PL model. This is not observed here.

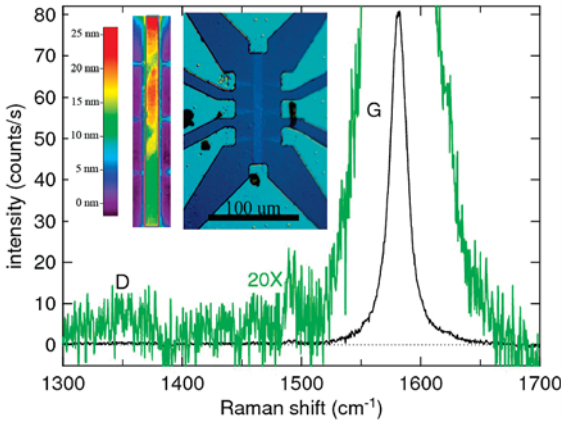

FIGURE 4. Raman scan showing D and G peaks of graphene in our devices. The signal is blown up by 20 times and overlaid onto the graph. The ratio of the peak intensities over the sample is used to determine an average grain size of ~1.5 μm. The inset shows a Nomarski image of a device and a Raman map of the device showing film thickness variations.

Despite the material's inhomogeneity and multilayer thickness, epitaxial multilayer graphene grown on SiC behaves as graphene rather than graphite. Past studies[20−24] have reported LMR was observed in large graphite crystals, but the LMR never survived to room temperature. Moreover, the LMR behavior previously observed in graphite was attributed mostly to impurities in the material or to parallel conductance.[20−24] Our material has been shown to have a negligible impurity concentration,[25] and parallel conductance has been ruled out as a cause for the observed behavior (see above). In addition, our material is fundamentally different from graphite because for C-face epitaxially grown films, graphene behavior is preserved independent of thickness. Weak interlayer interaction during growth leads to an interlayer separation and stacking order that is different from graphite.[26] Furthermore, it has been shown for C-face epitaxial graphene that the energy spectrum can be probed by far-infrared magneto-transmission (FIR-MT), and that for graphene the energy of the Landau absorption, $E \propto \sqrt{B}$, is indicative of massless carriers and linear energy dispersion.[27,28] Our samples show the same square-root B dependence in FIR-MT experiments.[29] Such experiments have also been performed on graphite films and square-root B dependence was not observed in those studies.[30]

To understand the origin of the observed LMR, we consider the two prevailing models, the classical PL model[11,13] and the quantum model.[1,2] We would expect, based on the structural composition of our sample, that the LMR behavior would be best explained by the classical PL model. Here, separate grains in the material act as a matrix of van der Pauw conductors. Inhomogeneities can cause scattering that leads to magnetotransport dominated by the size of the mobility fluctuations.[8,11] We, however, do not observe such mobility fluctuations. The PL model predicts that the crossover field, $H_c = \langle\mu\rangle^{-1}$, with $\langle\mu\rangle$ as the average mobility, should continually increase with increasing temperature due a decreasing average mobility.[11] We do not see such a change in H_c in Figure 3A, which remains somewhat constant in T. The PL model also predicts[4,11] that dMR(T)/dH $\propto \mu(T)$. Figure 3B displays a plot of dMR(T)/dH versus μ and H_c versus $1/\mu$. Neither data set can be fit linearly, demonstrating the PL model behavior is not realized in our system. Additionally, if the LMR was classical, then as the temperature is increased, we would expect the MR to increase by a power law, rather than the observed gradual increase displayed in Figure 2,[4,8] which rules out PL model behavior even at higher temperatures. Finally, the value of the crossover field does not shift as a function of temperature, which is expected for the classical case, as mobility fluctuations would dominate at higher temperatures. Thus, the graphene MR data cannot be explained by the classical model of LMR.

A better explanation for the observed LMR comes from the quantum model. At low temperature, where $\hbar\omega_c \gg k_B T$, $\hbar\omega_c$ can be greater than the Fermi energy. When these conditions are met, the lowest Landau band becomes highly degenerate, eventually resulting in direct proportionality between the MR and the applied transverse magnetic field termed the "extreme quantum limit" (EQL),[1,2,8] $\rho_{xx} \propto H$, $\rho_{xy} = RH$. Here, H is the applied transverse field, and R is the Hall coefficient. Our sample is in the EQL for low temperature, as evidenced by SdHO in Figure 1B. Moreover, the temperature condition for the EQL is[1,2] $T \ll eH\hbar/m^*c$; here m^* is the effective mass. For our graphene samples, $m^* \sim$

0, so the right-hand side of the inequality diverges making the EQL theoretically obtainable at room temperature and higher. Our data appear to follow the quantum model. However, we did not observe SdHO at higher temperatures, which may be due to limitations in our variable temperature equipment in measuring small signals at higher temperatures rather than the absence of quantum effects. Nevertheless, we are aware of no other materials that likely follow the Abrikosov model where the LMR effects survive up to room temperature. Despite the inhomogeneity in our devices, the quantum behavior likely dominates. Therefore, there must be some minimum amount of disorder necessary to observe these quantum effects, but it is also likely that too much disorder would destroy the EQL.

In conclusion, we have observed that LMR persists in C-face epitaxial graphene and 2.2 K and even up to room temperature. We attribute the observation of LMR to the large size of the devices compared to the size of the inhomogeneities, which allows the unmasking of the effect not observed in homogeneous (exfoliated) graphene. Our samples appear to remain in the EQL even to room temperature, in spite of predictions based on sample inhomogeneity that the classical PL model should account for LMR. Proper control and maximization of graphene device inhomogeneity in the future may result in further increases in the magnitude of these LMR effects. Avenues to control the graphene grain size during growth are currently being explored. This would allow tailoring of the degree of inhomogeneity to unmask the LMR, which could lead to new classes of giant or colossal quantum linear magnetoresistance devices for applications ranging from ultrahigh density memory storage to extremely sensitive linear motion sensors, which is especially true for those devices that would benefit from linearity, such as magnetic sensors.

Acknowledgment. The authors would like to thank Professor D. Heiman for helpful discussions. Work at the U.S. Naval Research Laboratory is support by the Office of Naval Research. J.K.H. and J.L.T. acknowledge the support of the American Society for Engineering Education/Naval Research Laboratory Postdoctoral Fellow Program. A.L.F. also acknowledges support from the National Research Council.

REFERENCES AND NOTES

(1) Abrikosov, A. A. *Phys. Rev. B* **1998**, *58*, 2788–2794.
(2) Abrikosov, A. A. *Europhys. Lett.* **2000**, *49*, 789–793.
(3) Husmann, A.; Betts, J. B.; Boebinger, G. S.; Migliori, A.; Rosenbaum, T. F.; Saboungi, M.-L. *Nature* **2002**, *417*, 421–424.
(4) Johnson, H. G.; Bennett, S. P.; Barua, R.; Lewis, L. H.; Heiman, D. *Phys. Rev. B* **2010**, *82*, 085202.
(5) Lee, M.; Rosenbaum, T. F.; Saboungi, M.-L.; Schnyders, H. S. *Phys. Rev. Lett.* **2002**, *88*, No. 06602.
(6) von Kreutzbruck, M.; Lembke, G.; Mogwitz, B.; Korte, C.; Janek, J. *Phys. Rev. B* **2009**, *79*, No. 035204.
(7) Xu, R.; Husmann, A.; Rosenbaum, T. F.; Saboungi, M.-L.; Enderby, J. E.; Littlewood, P. B. *Nature* **1997**, *390*, 57–60.
(8) Hu, J.; Rosenbaum, T. F. *Nat. Mater.* **2008**, *7*, 697–700.
(9) Delmo, M. P.; Yamamoto, S.; Kasai, S.; Ono, T.; Kobayashi, K. *Nature* **2009**, *457*, 1112–1116.
(10) Castro Neto, A. H.; Guinea, F.; Peres, N. M. R.; Novoselov, K. S.; Geim., A. K. *Rev. Mod. Phys.* **2009**, *81*, 109–162.
(11) Parish, M. M.; Littlewood, P. B. *Nature* **2003**, *426*, 162–165.
(12) Hu, J.; Parish, M. M.; Rosenbaum, T. F. *Phys. Rev. B* **2007**, *75*, 214203.
(13) Parish, M. M.; Littlewood, P. B. *Phys. Rev. B* **2005**, *72*, No. 094417.
(14) Novoselov, K. S.; Geim, A. K.; Morozov, S. V.; Jiang, D.; Katsnelson, M. I.; Grigorieva, I. V.; Dubonos, S. V.; Firsov, A. A. *Nature* **2005**, *438*, 197–200.
(15) Gaskill, D. K.; Jernigan, G. G.; Campbell, P. M.; Tedesco, J. L.; Culbertson, J. C.; VanMil, B. L.; Myers-Ward, R. L.; Eddy, C. R., Jr.; Moon, J.; Curtis, D.; Hu, M.; Wong, D.; McGuire, C.; Robinson, J. A.; Fanton, M. A.; Stitt, J. P.; Stitt, T.; Snyder, D.; Wang, X.; Frantz, E. *ECS Trans.* **2009**, *19*, 117–124.
(16) Tedesco, J. L.; VanMil, B. L.; Myers-Ward, R. L.; McCrate, J. M.; Kitt, S. A.; Campbell, P. M.; Jernigan, G. G.; Culbertson, J. C.; Eddy, C. R., Jr.; Gaskill, D. K. *Appl. Phys. Lett.* **2009**, *95*, 122102.
(17) Bruls, G. J. L.; Bass, J.; Van Gelder, A. P.; van kempen, H.; Wyder, P. *Phys. Rev. Lett.* **1981**, *46*, 553 (Shows how asymmetry in LMR measurements is an indicator of parallel conductance. Also eliminating parallel conductance in our sample were Hall mobility measurements that were constant in field and symmetric between contacts).
(18) Shivaraman, S.; Chandrashekhar, M. V. S.; Boeckl, J. J.; Spencer, M. G. *J. Electron. Mater.* **2009**, *38*, 725–730.
(19) Cancado, L. G.; Takai, K.; Enoki, T.; Endo, M.; Kim, Y. A.; Mizusaki, H.; Jorio, A.; Coelho, L. N.; Magalhaes-Paniago, R.; Pimenta, M. A. *Appl. Phys. Lett.* **2006**, *88*, 163106.
(20) McClure, J. W.; Spry, W. J. *Phys. Rev.* **1968**, *165* (3), 165.
(21) Soule., D. E. *Phys. Rev.* **1958**, *112* (3), 698.
(22) Wang, Z. M.; Xu, Q. Y.; Ni, G.; Du, Y. W. *Phys. Lett. A* **2003**, *314*, 328.
(23) Zhang, X.; Xue, Q. Z.; Zhu, D. D. *Phys. Lett. A* **2004**, *320*, 471.
(24) Morozov, S. V.; Novoselov, K. S.; Schedin1, F.; Jiang, D.; Firsov, A. A.; Geim, A. K. *Phys. Rev. B* **2005**, *72*, 201401.
(25) The major impurities in the substrate as measured by scanning ion mass spectroscopy are V and N (both about 10^{16} cm^{-3}); other impurity concentrations are Co (<10^{14} cm^{-3}), and Mn, Fe, Ni, and Cr (<0.01 to 0.05 ppm by weight). Private communication between D. K. Gaskill and I. Zwieback, II-VI, Inc., 2010.
(26) Sprinkle, M.; Soukiassian, P.; de Heer, W. A.; Berger, C.; Conrad, E. H. *Phys. Status Solidi RRL,* **2009**, *3* (6), A91–A94.
(27) Orlita, M.; Faugeras, C.; Plochocka, P.; Neugebauer, P.; Martinez, G.; Maude, D. K.; Barra, A.-L.; Sprinkle, M.; Berger, C.; de Heer, W. A.; Potemski, M. *Phys. Rev. Lett.* **2008**, *101*, 267601.
(28) Sadowski, M. L.; Martinez, G.; Potemski, M.; Berger, C.; de Heer, W. A. *Phys. Rev. Lett.* **2006**, *97*, 266405.
(29) Jernigan, G. G.; VanMil, B. L.; Tedesco, J. L.; Tischler, J. G.; Glaser, E. R.; Davidson, A., III; Campbell, P. M.; Gaskill, D. K. *Nano Lett.* **2009**, *9* (7), 2605–2609.
(30) Private communication from E. R. Glaser of the US Naval Research Laboratory; 2010.

DOI: 10.1021/nl101797d | *Nano Lett.* **XXXX,** *xxx,* 000–000